Theory and Experiments on the Stability of Robot Compliance Control

Brian J. Waibel and H. Kazerooni, *Member, IEEE*

Abstract—**This work presents a nonlinear stability analysis for constrained robotic motion, a maneuver where the manipulator contacts the environment. The external disturbances, sensor noises, parameter uncertainties, and the dynamics of the total system comprised of the robot and the environment have been modeled. The control of the manipulator is divided into two components: a computed torque trajectory controller that regulates the robot position and a compliance controller that modulates contact forces. Three sufficient conditions for stability have been derived. The first condition guarantees the stability of the system of robot and finite stiff environment when no force sensor and, consequently, no force feedback is considered for the system. The second condition guarantees stability of the robot and environment when a compliance compensator (operating on the contact force) supplements the trajectory controller. For a fixed trajectory controller, this criterion shows that the L_∞ gain of the compliance controller must vary in inverse proportion to the environment stiffness in order to guarantee stability. This criterion also shows that stability of the compliance compensator cannot be guaranteed when the robot operates near a singular point. The third stability criterion shows that, for a robot contacting a very stiff environment, the gain of the compliance compensator must vary in inverse proportion to the gain of the trajectory compensator.**

Nomenclature

$\theta_d, \dot{\theta}_d, \ddot{\theta}_d$	Command trajectory, velocity, and acceleration in joint space.
n	Degrees of freedom for manipulator.
$K(s)$	Laplace transform of trajectory compensator.
$M, \bar{M}$	Actual and model of the robot inertia matrix.
$C, \bar{C}$	Actual and model of coriolis, centrifugal, and gravitational forces.
τ_d, $N\tau$	Torque disturbance and its L_∞ bound.
$J(\theta)$	Jacobian matrix.
$I, 0$	Identity matrix and zero matrix.
u	Forces/torques applied by manipulator's actuators.
$\theta, \dot{\theta}, \ddot{\theta}$	Joint positions, velocities, and acceleration.
p	System state measurement error vector.
q	$[\theta \quad \dot{\theta}]^T$.
q_e	Command trajectory comprised of desired joint position and velocity $[\theta_d^T \quad \dot{\theta}_d^T]^T$.
H	Laplace transform of compliance compensator.
e, ϕ	Input signal for and output signal from trajectory compensator.
x, x_0	Position and velocity of manipulator endpoint and of the environment.
Kin	Mapping from q to x.
E	Environment function mapping environment deflection to contact force.
f, m	Contact force and its measurement noise.
A, B	Matrix coefficients for manipulator's state space linear dynamics.
D	Laplace transform of manipulator's linear dynamics.
ΔC	Quantity representing modeling error in the coriolis and centrifugal forces.
μ, ξ	Signal representing the nonlinear and modeling errors of the manipulator dynamics.
T, S	Transfer function matrices derived from the manipulator's linear dynamics.
α_T, α_S	$\hat{A}$ norm of T and S.
α_M	Bound on model for the inertia matrix.
α_{M1}, α_{M2}	Bounds on M^{-1} and $M^{-1}\bar{M} - I$.
$\alpha_{E1}, \alpha_{E1}, \beta_E$	Bounds on the environment dynamics.
$\alpha_{Kin}, \beta_{Kin}$	Bounds on the forward kinematics.
α_{JI}	Bounds on the inverse Jacobian.
$\Delta x, \Delta\theta$	Output from compliance compensator and signal from compliance control loop.
Δq	Compliance compensator result which is subtracted from command trajectory.

Manuscript received February 5, 1988; revised May 9, 1990.

B. J. Waibel is with Waibel Technical Computing, Newark, DE 19716.
H. Kazerooni is with the Mechanical Engineering Department, University of Minnesota, Minneapolis, MN 55455.

IEEE Log Number 9041038.

I. Introduction

APPLICATION of robotics to manufacturing tasks requires mechanical interaction with the environment or with the object being handled, in addition to high-speed maneuvering in unconstrained space. For example, in a robotic assembly task whose objective is combining a number of individual parts into one completed device, the parts must be quickly assembled while avoiding damage to either the individual parts or the device. The very nature of the assembly process requires the robot (through the part) to contact the environment (the partially completed device). To successfully complete this constrained maneuver, the manipulator must develop compliant motion where the interaction force[1] along the constrained direction is accommodated rather than resisted.

Whitney [21] identifies six different approaches for robot force control. These six may be divided into two categories of compliant motion development: hybrid control and compliance control. The hybrid control method controls force and position in a nonconflicting way [13]–[16], [18] commanding force along directions constrained by the environment and position along those directions in which the manipulator is unconstrained. The compliance control approach focuses on the relationship between the manipulator position, the commanded quantity, and the interaction force, a specified function of the command signal [4], [6], [7], [12], [17]. With this approach, the designer can ensure that the manipulator will maneuver in a constrained space while maintaining an appropriate contact force.

[1] The term "force" implies both forces and torques. Position, in a Cartesian sense, implies both position and orientation.

1042-296X/91/0200-0095$01.00

This work represents a synthesis and extension of the stability analysis of Spong and Vidyasagar [19] and the compliance control analysis in Kazerooni *et al.* [9]. Spong and Vidyasagar model the dynamics of a robot performing unconstrained manipulation and derive a criterion for closed-loop trajectory control stability in light of parameter uncertainties, external disturbances, and sensor noise. Kazerooni *et al.* define a compliance controller and derive a nonglobal stability condition for manipulation interaction with an infinitely stiff environment. Other approaches in stability analysis of compliant motion control can be found in [1]–[3], [5], [8].

We are concerned with the global stability of a manipulator interacting with an environment. We apply the analysis of [19] to both the manipulator and environment dynamics and derive global stability conditions for the system taken as a whole. The mathematical conventions and nomenclature of this paper are contained in Appendix A. Section II describes the manipulator dynamic behavior, and Section III models the dynamics behavior of a finite stiffness environment. Section IV analyzes the manipulator interaction with a finite stiffness environment and derives a stability condition from which the stability results of [19] can be obtained as a special case. Section V defines a compliance feedback controller to modulate the interaction with a finite stiffness environment. Section VI differentiates between finite and infinite stiffness environments and derive, for an infinite stiffness environment, a stability condition analogous to that in Section V.

II. Manipulator Dynamics

The dynamic behavior of a direct drive robot with n degrees of freedom can be expressed by

$$M(\theta)\ddot{\theta} + C(\theta, \dot{\theta}) = u + \tau_d - J^T(\theta) f. \tag{1}$$

There are three inputs to the robot dynamics: the actuator torques,[2] u; a disturbance torque τ_d and the applied forces f acting at the endpoint and transformed into joint forces via the Jacobian transpose matrix $J^T(\theta)$. The Jacobian $J(\theta)$ is assumed to be a square matrix.[3] The disturbance torque τ_d is a function solely dependent on time that encompasses all exogenous inputs. While this might, in many cases, be difficult to model, it is assumed that, for the purposes of stability analysis, the L_∞ norm of τ_d is bounded such that $\|\tau_d\|_\infty \triangleq \alpha_{\tau d} < \infty$.[4] Notice that if the disturbance torque τ_d and the applied force f are zero, the system may be an unstable function of the actuator torque, i.e. a finite torque may cause the joint positions to grow unboundedly.

Based on the manipulator dynamics of (1), a trajectory controller is chosen to stabilize the nonlinear dynamics of the robot manipulator. This trajectory controller requires some information about the robot's position θ and joint velocities $\dot{\theta}$. Together, these quantities represent the manipulator's states, which we denote by the $2n$ vector $q \triangleq [\theta, \dot{\theta}]^T$. q represents the actual system states, but only the measured states are available for the controller. It is assumed that the measured system states are $q + p$, where q is the actual system states and p represents the $2n$ vector of measurement noise. To support the stability analysis, the measurement error p is assumed to be a Lebesque measurable function[5] and its L_∞ norm is bounded such that $\|p\|_\infty \triangleq \alpha_p < \infty$.

Using the "computed torque method," a model-based control scheme, the input torque u is defined as

$$u = \bar{M}[\ddot{\theta}_d + \phi] + \bar{C} \tag{2}$$

where $\bar{M}$ and $\bar{C}$ are the nominal models for M and C. These models are either derived experimentally or analytically. $\ddot{\theta}_d$ is the feedforward, joint space command acceleration. ϕ is the output signal from the linear trajectory compensator and is defined as

$$\phi = K^*\{q_e - q - p\} \tag{3}$$

where $\phi = K^*\{q_e - q - p\}$ denotes the convolution of the impulse response of $K(s)$ with the signal $q_e - q - p$, q_e is a $2n$ vector function for the command position and velocity, and $K = [K_P \quad K_V]$; K_P and K_V are, in general, stable transfer function matrices. For a proportional-derivative trajectory controller, K_P and K_V are constant, diagonal matrices. K is an L_∞-stable function of its input such that $K(\cdot)$: $L_\infty^{2n} \to L_\infty^n$ and

$$\|\phi\|_\infty \le \alpha_K(\|q_e\|_\infty + \|q\|_\infty + \|p\|_\infty), \quad \forall q_e, q \text{ and } p \in L_\infty^{2n} \tag{4}$$

where α_K denotes the $\hat{A}$ norm of K. (See Appendix A.) Substituting (2) into (1) results in (5) where ϕ represents the output of the robot's linear trajectory compensator, and a signal μ represents the output of all the nonlinear and feedforward dynamics.

$$\ddot{\theta} = \phi + \mu \tag{5}$$

where

$$\mu = [M^{-1}\bar{M} - I]\phi + M^{-1}\Delta C + M^{-1}\tau_d + M^{-1}\bar{M}\ddot{\theta}_d - M^{-1}J^T f \tag{6}$$

and $\Delta C = \bar{C} - C$. The first two terms of μ, which express the modeling error, are functions of the system states q while the last term in μ shows the contribution of the manipulator-environment contact force to the system dynamics. The modeling errors are defined by ξ in (7).

$$\xi = [M^{-1}\bar{M} - I]\phi + M^{-1}\Delta C. \tag{7}$$

It is assumed the modeling errors in the system are bounded such that

$$\|M^{-1}\bar{M} - I\|_\infty \triangleq \alpha_{M1} < \infty, \qquad \forall \theta \in R^n \tag{8}$$

$$\|\Delta C\|_\infty \triangleq \alpha_{\Delta C} < \infty, \qquad \forall \theta \text{ and } \dot{\theta}_d \in R^n. \tag{9}$$

It is also assumed that the command trajectory is bounded such that $\|q_e\|_\infty \triangleq \alpha_{qe} < \infty$ and $\|\ddot{\theta}_d\|_\infty \triangleq \alpha_{\ddot{\theta}d} < \infty$. The lemma of Appendix B demonstrates that ξ is an L_∞ stable function of q under the above conditions such that $\xi(\cdot)$: $L_\infty^{2n} \to L_\infty^n$ and also there exist positive constants α_ξ and β_ξ such that

$$\|\xi\|_\infty \le \alpha_\xi \|q\|_\infty + \beta_\xi, \qquad \forall q \in L_\infty^{2n}. \tag{10}$$

[2] Unless otherwise noted, all matrices are $n \times n$ and all vectors are $n \times 1$. Hereafter, the arguments for all functions will be omitted except when new quantities are defined or when required for clarity.

[3] The solution of differential equation (1) when u, f, τ_d are finite is defined as the robot workspace. This implicitely eliminates any point that $J(\theta)$ is singular.

[4] The symbol $\triangleq$ means "is defined as."

[5] All functions based on physical systems can be safely assumed, for practical purposes, to be Lebesque measurable. Hereafter, when discussing bounds on a function, we implicitly assume that the function is Lebesque measurable.

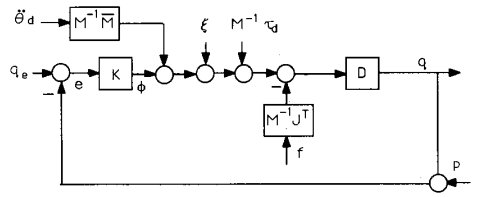

Fig. 1. Dynamic model for the robot interacting with a trajectory controller. Although ξ is a function of the system states and other parameters, the feedback pathways have been omitted for clarity.

Using the state vector q, (5) may be expressed as a state differential equation

$$\dot{q} = Aq + B[\phi + \mu] \tag{11}$$

where

$$A = \begin{bmatrix} 0 & I \\ 0 & 0 \end{bmatrix} \quad \text{and} \quad B = \begin{bmatrix} 0 \\ I \end{bmatrix}. \tag{12}$$

By considering (12) to be a linear equation where q is the output and $[\phi + \mu]$ is the input, the $2n \times 2n$ transfer function matrix for the system is given by

$$D(s) = [sI - A]^{-1}B. \tag{13}$$

Using the convention defined in Appendix A, the relationship in (13) may be rewritten as

$$q = D^*\{\phi + \mu\}. \tag{14}$$

The block diagram in Fig. 1 represents the dynamic behavior of the manipulator and trajectory controller.

Equation (14) is a state space differential equation written in terms of the manipulator's position and velocity states and differs from the error equation typically employed in the stability analysis of robot trajectory controllers [19]. To analyze the tracking performance in unconstrained manipulation, (14) would typically be written in terms of the tracking error, i.e., the difference between the command trajectory and the physical trajectory. Because the interaction with the environment is directly related to the physical states and not the tracking error, (14) leads to a clearer stability analysis for trajectory control in constrained maneuvering, and, moreover, it provides a convenient basis for stability analysis when an additional feedback loop is added around the trajectory controller to tailor the system compliancy.

III. Environment Dynamics and Its Interaction with the Manipulator

The first component of the manipulator-environment interaction is the transformation from joint space quantities to Cartesian space quantities. x is defined to be a $2n \times 1$ vector representing the manipulator's Cartesian endpoint position and velocity in the global coordinate frame. Equation (15) represents the mapping from the joint space to Cartesian space.

$$x = Kin(q) \tag{15}$$

$Kin(\cdot)$ is comprised of the manipulator's forward kinematics functions and Jacobian. It is assumed that $Kin(\cdot)$ is L_∞ stable such that $Kin(\cdot)$: $L_\infty^{2n} \to L_\infty^{2n}$, and there exist positive constants α_{Kin} and β_{Kin} such that

$$\|x\| \le \alpha_{Kin}\|q\| + \beta_{Kin}, \qquad \forall q \in L_\infty^{2n}. \tag{16}$$

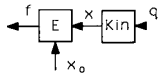

Fig. 2. Block diagram illustrating the mapping from the system states q to the interaction force f. f and x are measured relative to the same global coordinate frame.

When the manipulator comes into contact with an environment of finite stiffness, a displacement of the environment's surface results in an interaction force. It is assumed that the environment displacement and the contact force are measured in the global coordinate frame. The relationship between the environment's displacement and interaction force is referred to as the environment impedance. Intuitively, this impedance will be a large quantity when the environment is very "stiff" in some directions and a small quantity when the environment is very "soft" in all directions. The environment dynamics is defined as

$$f = E(x, x_0) \tag{17}$$

where x_0 is a $2n$ vector representing the initial position and velocity of the environment before manipulator-environment contact. E may be loosely thought of as the stiffness of the environment, though E may represent either a linear or nonlinear relationship. For situations where the manipulator can interact with the environment only in some directions, the E mapping will be singular, meaning that the component of f in the unconstrained directions is zero for all displacements x. For example, in contacting a surface, the robot is constrained in the normal direction but is free to move in the two tangential directions. It is assumed that the environment is L_∞ stable such that $E(\cdot)$: $L_\infty^{2n} \times L_\infty^{2n} \to L_\infty^n$, and there exist positive constants α_{E1}, α_{E2}, and β_E such that

$$\|f\|_\infty \le \alpha_{E1}\|x\|_\infty + \alpha_{E2}\|x_0\|_\infty + \beta_E, \qquad \forall x \text{ and } x_0 \in L_\infty^{2n}. \tag{18}$$

Using the convention for transfer functions defined in Appendix A, the output force $f = E(x - x_0)$ equals the convolution of the environment's impulse response and the vector $x - x_0$. In this case, α_{E1} would be the $\hat{A}$ norm of E, $\alpha_{E2} = \alpha_{E1}$, and $\beta_E = 0$. Fig. 2 summarizes the manipulator's kinematics, manipulator-environment interaction, and the environment dynamics in block diagram form.

By taking the composition of the kinematics mapping $Kin(\cdot)$, in (15) and the environment dynamics E in (17), the mapping from q to f is defined by

$$f = E(Kin(q), x_0). \tag{19}$$

The L_∞ norm of both sides of (19) is found by substituting inequality (16) into inequality (18)

$$\|f\|_\infty \le \alpha_{E1}\alpha_{Kin}\|q\|_\infty + \alpha_{E2}\|x_0\|_\infty + \alpha_{E1}\beta_{Kin} + \beta_E. \tag{20}$$

Inequality (20) defines the L_∞ bound on the mapping from q to f.

IV. Robot-Environment Interaction without the Use of Force Sensors

This section describes the stability of the robot manipulator and environment taken as a whole when no force sensor is used in measurement of the contact force. The block diagram of Fig. 3 is derived from (3), (6), (7), (14), (15), and (17). The linear

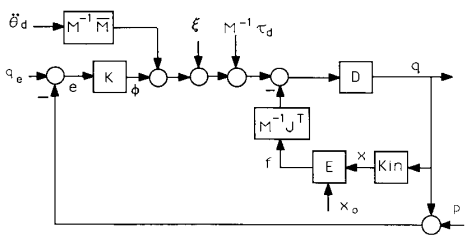

Fig. 3. Detailed block diagram showing the components of the combined manipulator and environment system. While the nonlinear modeling error ξ is a function of the system states, command trajectory, and measurement noise, the feedback pathways have been omitted for clarity.

trajectory compensator, represented by K, receives the tracking error as an input and delivers the output ϕ to the manipulator.

By inspection of Fig. 1, we define the system states with the following vector function:

$$q = S\{\xi - M^{-1}J^T f + M^{-1}\tau_d + M^{-1}\bar{M}\ddot{\theta}_d\} + T\{q_e - p\} \tag{21}$$

where T and S are stable transfer function matrices defined by

$$S = [I + DK]^{-1}D$$
$$T = [I + DK]^{-1}DK \tag{22}$$

Let α_T and α_S denote the $\hat{A}$ norm of the T and S functions, respectively. These values represent the L_∞ gain of T and S, respectively. To arrive at the stability of the closed loop system of Fig. 3, the truncated L_∞ norm of q is derived from (21).

$$\begin{aligned}\|q\|_{T\infty} \le{}& \alpha_S\|\xi\|_{T\infty} + \alpha_S\alpha_{M2}\alpha_J\|f\|_{T\infty} \\ &+ \alpha_S\|M^{-1}\tau_d + (M^{-1}\bar{M} - I)\ddot{\theta}_d + \ddot{\theta}_d\|_{T\infty} \\ &+ \alpha_T\|q_e - p\|_{T\infty}, \qquad \forall t \in [0, T]\end{aligned} \tag{23}$$

where, for all possible θ, $\|J^T\|_\infty \triangleq \alpha_J < \infty$ and $\|M^{-1}\|_\infty \triangleq \alpha_{M2} < \infty$. Only ξ and f may be unbounded functions of q. Substituting for $\|\xi\|_{T\infty}$, $\|f\|_{T\infty}$, $\|\tau_d\|_{T\infty}$, $\|(M^{-1}\bar{M} - I)\|_{T\infty}$ and $\|\ddot{\theta}_d\|_{T\infty}$ into inequality (23) results in inequality (24).

$$\begin{aligned}\|q\|_{T\infty} \le{}& \alpha_S(\alpha_\xi + \alpha_{M2}\alpha_J\alpha_{E1}\alpha_{Kin})\|q\|_{T\infty} \\ &+ \alpha_S(\beta_\xi + \alpha_{M2}\alpha_J\alpha_{E1}\beta_{Kin} \\ &+ \alpha_{M2}\alpha_J\alpha_{E2}\alpha_{x0} + \alpha_{M2}\alpha_J\beta_E) \\ &+ \alpha_S(\alpha_{M2}\alpha_{\tau d} + \alpha_{M1}\alpha_{\ddot{\theta}d} + \alpha_{\ddot{\theta}d}) + \alpha_T\alpha_{qe} + \alpha_T\alpha_p, \\ &\forall t \in [0, T]\end{aligned} \tag{24}$$

where $\|x_0\|_\infty \triangleq \alpha_{x0} < \infty$. Rearranging inequality (24) results in inequality (25).

$$\begin{aligned}&(1 - \alpha_S(\alpha_\xi + \alpha_{M2}\alpha_J\alpha_{E1}\alpha_{Kin}))\|q\|_{T\infty} \\ &\le +\alpha_S(\beta_\xi + \alpha_{M2}\alpha_J\alpha_{E1}\beta_{Kin} \\ &\quad + \alpha_{M2}\alpha_J\alpha_{E2}\alpha_{x0} + \alpha_{M2}\alpha_J\beta_E) \\ &\quad + \alpha_S(\alpha_{M2}\alpha_{\tau d} + \alpha_{M1}\alpha_{\ddot{\theta}d} + \alpha_{\ddot{\theta}d}) + \alpha_T\alpha_{qe} + \alpha_T\alpha_p, \\ &\quad \forall t \in [0, T].\end{aligned} \tag{25}$$

The right-hand side of inequality (25) has already been established as bounded quantities $\forall t \in [0, \infty)$; therefore, the closed-loop system of Fig. 3 is L_∞ stable if inequality (26) is satisfied.

$$\alpha_S(\alpha_\xi + \alpha_{M2}\alpha_J\alpha_{E1}\alpha_{Kin}) < 1. \tag{26}$$

Inequality (26) is a sufficient condition for stability of the closed-loop system shown in Fig. 3. If this inequality is satisfied, the trajectory-controlled robot is guaranteed stability when interacting with a finite stiffness environment. If inequality (26) is not satisfied, no conclusions can be made. This stability criterion shows the relative contribution of the linear trajectory compensator, modeling error, manipulator dynamics, and environment dynamics to the system stability.

Furthermore, a manipulator performing unconstrained manipulation is equivalent to a manipulator interacting with an environment having zero stiffness ($\alpha_{E1} = 0$). The trajectory control stability criterion then reduces to

$$\alpha_S\alpha_\xi < 1. \tag{27}$$

Inequality (27) shows that, to guarantee the system stability, the system sensitivity α_S must decrease in inverse proportion to the modeling error α_ξ. α_S shows the sensitivity of the system to modeling error and external forces operating on the robot and is directly related to the linear trajectory compensator. Roughly speaking, the gain α_S varies as the inverse of the position gain K_P in the trajectory compensator; thus, the manipulator will have small sensitivity if K_P is large and vice versa. α_ξ is a measurement of the nonlinear modeling error and approaches zero as the nominal model for the manipulator dynamics approaches the actual manipulator dynamics. For a system with a PD trajectory compensator and a large α_ξ, the position gain K_P must be large in order to provide the small sensitivity α_S needed to guarantee stability. Because robots, in general, perform both unconstrained and constrained maneuvers during their normal operation, inequalities (27) and (26) must both be satisfied to guarantee stability for all possible maneuvers.

In many situations, in particular in contact with a stiff environment, $\alpha_{M2}\alpha_J\alpha_{E1}\alpha_{Kin} \gg \alpha_\xi$ such that the modeling error can be assumed zero. The stability condition (26) can be written as

$$\alpha_S\alpha_{E_1} < \frac{1}{\alpha_{M2}\alpha_J\alpha_{Kin}}. \tag{28}$$

Inequality (28) shows that the system sensitivity must vary as the inverse of the environment stiffness to guarantee the system stability. $\alpha_{M2}\alpha_J$ and α_{Kin} are measures of the manipulator's dynamics and kinematics, respectively, and are fixed for a particular robot mechanism. α_{E1} is a measure of the environment dynamics.

The sum within inequality (26) shows the relative contribution of the interaction loop gain and the modeling error to the system stability. In order to guarantee stability, the system sensitivity must decrease as the environment stiffness increases and vice versa. This implies that K_p and K_v must be small when contacting the environment.

V. Robot–Environment Interaction with Force Feedback

We propose to modulate the contact force between the manipulator and environment by adding a compliance compensator that alters the command trajectory as a function of the measured contact force. Fig. 4 shows the block diagram of a compliance-controlled robot interacting with a finite stiffness environment. The compliance controller receives the noise-corrupted interac-

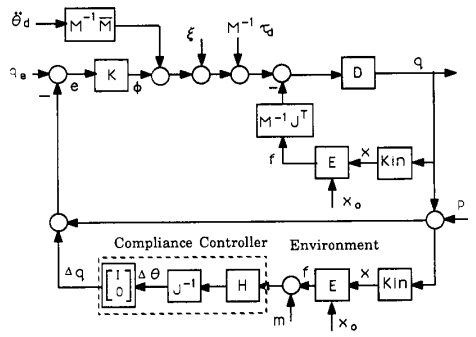

Fig. 4. H, a stable transfer function matrix, may be chosen by the designer to produce the desired system compliancy. The matrix following the inverse Jacobian J^{-1} is a $2n \times n$ matrix, where I is an $n \times n$ identity matrix and 0 is an $n \times n$ null matrix, and indicates that the compliance controller only modulates the command position. The noise in the force measurement is represented by the vector m.

tion force $f + m$ as an input and delivers a vector $\Delta\theta$ that modulates the command trajectory

$$\Delta\theta = J^{-1}H^*\{f + m\} \tag{29}$$

where J^{-1} is the inverse Jacobian matrix and H is the compliance compensator, a transfer function matrix. Here we implicitely assume that the robot does not travel through the singular points where J^{-1} does not exist. The motivation for this choice is that this compliance feedback loop supplements the compliancy resulting from the natural loop by placing a servo on the contact force.

The compliance controller H in Fig. 4 modulates the command trajectory q_e as a function of the measured contact force $f + m$. The output of the compliance compensator $\Delta\theta$ is transformed into Δq by a constant $2n \times n$ matrix containing the identity and a null submatrix. By inspection of Fig. 4, Δq is computed by

$$\Delta q = \begin{bmatrix} I & 0 \end{bmatrix}^T J^{-1}H^*\{f + m\} \tag{30}$$

where f is given by (19). Appendix C shows that if the robot does not maneuver around its singular region and H is stable, then mapping in (30) is an L_∞ stable function of q such that

$$\|\Delta q\|_\infty \le \alpha_{\Delta q}\|q\|_\infty + \beta_{\Delta q}, \qquad \forall q \in L_\infty^{2n}. \tag{31}$$

To derive the stability criterion of the system of Fig. 4, one requires an expression for the system states q as a function of the system inputs. Since Fig. 4 represents a modification of the block diagram in Fig. 3, an expression for q that takes the contribution of Δq into consideration may be obtained through modification of (21).

$$q = S\{\xi - M^{-1}J^Tf + M^{-1}\tau_d + M^{-1}\bar{M}\ddot{\theta}_d\} + T\{q_e - p - \Delta q\}. \tag{32}$$

The truncated L_∞ norm of (32) is written as

$$\begin{aligned}\|q\|_{T\infty} \le{}& \alpha_S\|\xi\|_{T\infty} + \alpha_s\alpha_{M2}\alpha_J\|f\|_{T\infty} \\ &+ \alpha_S\|M^{-1}\tau_d + M^{-1}\bar{M}\ddot{\theta}_d\|_{T\infty} \\ &+ \alpha_T\|q_e - p - \Delta q\|_{T\infty}, \\ &\forall t \in [0, T]\end{aligned} \tag{33}$$

substituting for all the bounds and rearranging the terms in (33) similar to an inequality derivation of inequality (25) yields

$$\begin{aligned}&\left(1 - \alpha_S(\alpha_\xi + \alpha_{M2}\alpha_J\alpha_{E1}\alpha_{Kin} + \alpha_T\alpha_{\Delta q})\right)\|q\|_{T\infty} \\ &\quad\le +\alpha_S(\beta_\xi + \alpha_{M2}\alpha_J\alpha_{E1}\beta_{Kin} \\ &\qquad+\alpha_{M2}\alpha_J\alpha_{E2}\alpha_{x0} + \alpha_{M2}\alpha_J\beta_E) \\ &\qquad+ \alpha_S(\alpha_{M2}\alpha_{\tau d} + \alpha_{M1}\alpha_{\ddot{\theta}d} + \alpha_{\ddot{\theta}d}) \\ &\qquad+ \alpha_T\alpha_{qe} + \alpha_T\alpha_p + \alpha_T\beta_{\Delta q}, \qquad \forall t \in [0, \infty)\end{aligned} \tag{34}$$

where $\|J^{-1}\|_\infty \triangleq \alpha_{JI} < \infty$. The right-hand side of inequality (34) has already been established as bounded quantities $\forall t \in [0, \infty)$; therefore, the closed loop system of Fig. 4 is L_∞ stable if inequality (35) is satisfied.

$$\alpha_S\alpha_\xi + \alpha_S\alpha_{M2}\alpha_J\alpha_{E1}\alpha_{Kin} + \alpha_T\alpha_{\Delta q} < 1. \tag{35}$$

Substituting $\alpha_{\Delta q}$ from Appendix C yields

$$\alpha_S\alpha_\xi + (\alpha_S\alpha_{M2}\alpha_J + \alpha_T\alpha_{JI}\alpha_H)\alpha_{E1}\alpha_{Kin} < 1. \tag{36}$$

This inequality is a sufficient condition to guarantee the stability of the compliance-controlled manipulator shown in Fig. 4. If inequality (36) is satisfied, then the system shown in Fig. 4 is guaranteed to be stable; if this condition is not satisfied, no conclusion may be drawn. Note that the stability criterion in inequality (36) reduces to stability criterion of (26) if the gain of the compliance compensator α_H is zero. The key difference between the two criteria is that the stability criterion contains the sum of the compliance controller gain with the gain of the system sensitivity α_s.

If the modeling error gain $\alpha_s\alpha_\xi$ is small, then

$$(\alpha_S\alpha_{M2}\alpha_J + \alpha_T\alpha_{JI}\alpha_H)\alpha_{E1}\alpha_{Kin} < 1. \tag{37}$$

This inequality shows the relative contribution of the compliance compensator, manipulator dynamics and kinematics, trajectory compensator, and environment dynamics to the stability of the compliance-controlled robot interacting with a finite-stiffness environment. The manipulator dynamics and kinematics are fixed for a particular manipulator design; hence, $\alpha_{M2}\alpha_J$ and α_{Kin} may not be varied. For a fixed trajectory compensator, inequality (37) shows that, as the environment stiffness increases, the gain of the compliance compensator α_H must decrease and vice versa. This inequality also demonstrates that stability cannot be guaranteed when the manipulator operates in the vicinity of a single point, where the maximum singular value of the inverse Jacobian α_{JI} approaches infinity. In addition, for a given environment, the impact of the trajectory compensator K on the compliance compensator H cannot be clearly assessed because both α_S and α_T are a function of the trajectory compensator; these conclusions can be obtained through calculation of α_S, α_T, and α_H for a particular trajectory compensator and compliance compensator.

VI. Stability Analysis for Robot Interaction with an Infinite Stiffness Environment

In many manufacturing situations such as robot deburring, the manipulator is likely to encounter an environment whose stiffness is much greater than that of the manipulator's mechanism or controller. In the case of a very stiff environment, the environment acts as a kinematic constraint on the robot, which means that the environment dictates the trajectory (position, velocity, etc.) of the manipulator endpoint. In this case, inequal-

ity (18) will not be valid because a finite environment stiffness α_{E1} cannot be defined. The analysis that follows does not contain the environment dynamic model E. Moreover, the transient period from unconstrained to constrained manipulation is ignored. This assumption implies that the manipulator experiences no impact forces during its maneuvers. Equation (1) can be rewritten as

$$f = J^{-T}\left[u - M\ddot{\theta} - C + \tau_d\right]. \tag{38}$$

ϕ is modified to include the compliance controller H of (30). Substituting the new ϕ in control law of (2) results in (39).

$$u = \bar{M}\ddot{\theta}_d + \bar{M}K*\{-[I \;\; 0]^T J^{-1} H*\{f + m\} + q_e - q - p\} + \bar{C}. \tag{39}$$

Substituting (39) in (38) leads to an expression for the contact force for a manipulator interacting with an infinitely stiff environment

$$\begin{aligned} f = & -J^{-T}\bar{M}K[I \;\; 0]^T J^{-1} H*\{f\} \\ & + J^{-T}\left[\bar{M}K*\{q_e - q - p\} + \bar{M}\ddot{\theta}_d - M\ddot{\theta} + \Delta C + \tau_d\right] \\ & - J^{-T}\left[\bar{M}K*\{[I \;\; 0]^T J^{-1} H*\{m\}\}\right]. \end{aligned} \tag{40}$$

The command acceleration $\ddot{\theta}_d$, command trajectory q_e, states measurement noise p, force measurement noise m, and disturbance torque τ_d are all not a function of f. The system states q and the manipulator acceleration $\ddot{\theta}$ are dictated by the environment; we denote these two quantities by q_0 and $\ddot{\theta}_0$ and also $\|q_0\|_\infty \triangleq \alpha_{q0} < \infty$, $\|\ddot{\theta}_0\|_\infty \triangleq \alpha_{\ddot{\theta}0} < \infty$. Note that $\|J^{-1}\|_\infty = \|J^{-T}\|_\infty$ and the bound on their quantities is α_{JI}. In a particular direction, the manipulator is either constrained by the environment or unconstrained. Along those directions which the environment constrains the manipulator, the environment dictates the manipulator's position, velocity, etc. Along those directions unconstrained by the environment, the robot is performing unconstrained manipulation, and, as a direct result of the assumed stability in unconstrained maneuvers, the joint position and its derivatives are L_∞-bounded quantities. Although the position and velocity may be bounded, the contact force may be unbounded.

The stability of a robot interacting with an infinitely stiff environment is determined by taking the truncated L_∞ bound of both sides of (40).

$$\begin{aligned} \|f\|_{T\infty} \le & \|J^{-T}\bar{M}K[I \;\; 0]^T J^{-1} H*\{f\}\|_{T\infty} \\ & + \|J^{-T}\left[\bar{M}K*\{q_e - q - p\} + \bar{M}\ddot{\theta}_d - M\ddot{\theta} + \Delta C + \tau_d\right]\|_{T\infty} \\ & + \|J^{-T}\left[\bar{M}K*\{[I \;\; 0]^T J^{-1} H*\{m\}\}\right]\|_{T\infty}, \\ & \forall t \in [0, t]. \end{aligned} \tag{41}$$

Assuming $\|\bar{M}\|_\infty \triangleq \alpha_M < \infty$ and rearrangements of the terms of inequality (41), inequality (42) can be obtained.

$$\begin{aligned} & (1 - \alpha_{JI}\alpha_M\alpha_K\alpha_{JI}\alpha_H)\|f\|_{T\infty} \\ & \le \alpha_{JI}(\alpha_M\alpha_K(\alpha_{qe} + \alpha_{q0} + \alpha_p) \\ & \quad + \alpha_M\alpha_{\ddot{\theta}d} + \alpha_M\alpha_{\ddot{\theta}0} + \alpha_{\Delta C} + \alpha_{\tau d}) \\ & \quad + \alpha_{JI}\alpha_M\alpha_K\alpha_{JI}\alpha_H\alpha_m, \qquad \forall t \in [0, T]. \end{aligned} \tag{42}$$

Fig. 5. University of Minnesota Robot.

The right-hand side of inequality (42) has already been established as bounded quantities $\forall t \in [0, \infty)$; therefore, the closed-loop system of Fig. 4 when the environment is infinitely stiff is L_∞ stable if inequality (43) is satisfied.

$$\alpha_{JI}\alpha_M\alpha_K\alpha_{JI}\alpha_H < 1 \tag{43}$$

where α_M is the least upper bound on the maximum singular value of $\bar{M}$ for all possible joint positions, α_K is the L_∞ gain of the trajectory compensator K, and all other constants have the same, previously described meaning. Like the trajectory control and compliance control stability criteria, inequality (43) is a sufficient condition to guarantee the stability of the robot interacting with an infinitely stiff environment. If this inequality is satisfied, the system is guaranteed stable; if this condition is not satisfied, no conclusions may be made. Because we have ignored impact forces, this condition applies only during constrained maneuvers.

Like the previous two stability criteria, inequality (43) shows the relative contribution of the manipulator dynamics and kinematics, trajectory compensator, and compliance compensator to the system stability. This inequality shows that the gain of the compliance compensator α_K must vary in inverse proportion to the gain of the trajectory compensator α_K in order to guarantee stability. Moreover, the inequality shows that stability cannot be guaranteed when the manipulator operates near a singular point, where α_{JI} approaches infinity.

VII. Experimental Results

To demonstrate the stability criteria, a set of experiments was carried out on the University of Minnesota Robot. The experimental results verify inequality (43), the stability condition for a compliance-controlled robot interacting with an infinitely stiff environment.

The Minnesota Robot is a statically balanced, direct-drive, three-degree-of-freedom manipulator [10], [11]. The robot as well as the force-sensing apparatus are shown in Fig. 5. The joint position vector θ is equal to $[\theta_1, \theta_2, \theta_3]^T$, where θ_1, θ_2,

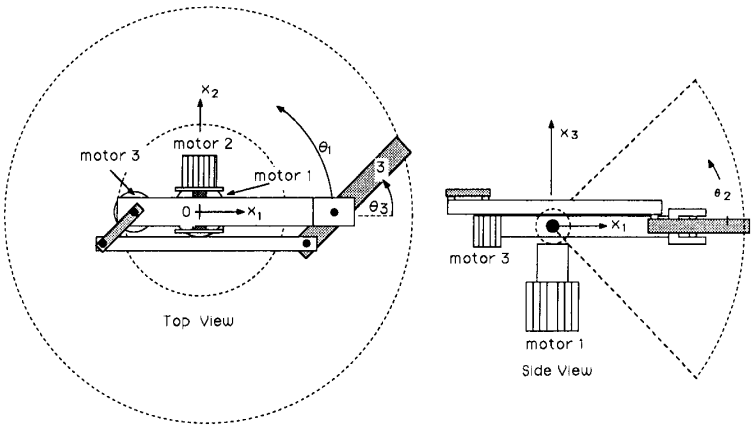

Fig. 6. Top and side views of the Minnesota Robot showing the manipulator workspace, the joint positions, and the global Cartesian reference. Note that if θ_2 is zero, the manipulator endpoint moves within the horizontal or $x_3 = 0$ plane.

and θ_3 are defined in Fig. 6. θ_1 indicates the angular position of motor 1 or the base motor; similarly, θ_2 and θ_3 indicate the positions of motor 2 and motor 3, respectively. The dynamic and kinematic equations for this robot are given in [10]. The endpoint position of the manipulator x is given as $x = [x_1 x_2 x_3]^T$, where the reference axes are shown in Fig. 6. Reference [10] also gives the analytically derived models for manipulator dynamics $\bar{M}$ and $\bar{C}$, the Jacobian, and the manipulator's kinematics *Kin*. Because the Minnesota Robot is statically balanced, the gravity force is zero for all possible configurations.

The bounds α_M and α_{JI} were computed numerically. $\bar{M}$ and J^{-1} are given in [10]. For any given θ, the $\bar{M}$ and J^{-1} become constant real valued matrices. The maximum and minimum singular values of $\bar{M}$ and J^{-1} were computed over a finite number of positions θ, evenly spaced throughout the robot workspace. α_M and α_{JI} were taken as the maximum singular values

$$\|\bar{M}\|_\infty \triangleq \alpha_M < 2.86 \text{ kg} \cdot \text{m}^2$$
$$\|J^{-1}\|_\infty \triangleq \alpha_{JI} < 13.82 \text{ rad/m}.$$

With the bounds on the nonlinear system dynamics established, the bounds on the linear system dynamics and the trajectory compensator can be determined. The trajectory compensator K and the robot's linear transfer function D are both diagonal matrices. If we focus on the position states of the system, D reduces to a 2×2 matrix of double integrators.

$$D = \frac{1}{s^2} I. \tag{44}$$

Choosing $K = [K_p \quad K_v] = [100 \quad 10]$, the $\hat{A}$ norms of S, T, and K were analytically determined, in each case, by taking the inverse Laplace transform of the respective transfer function and applying the definition of the $\hat{A}$ norm given in Appendix A.

$$\alpha_S = \|[I + DK]^{-1} D\|_{\hat{A}} = \frac{1}{K_p}$$
$$\alpha_T = \|[I + DK]^{-1} DK\|_{\hat{A}} = 1.0$$
$$\alpha_K = \|K\|_{\hat{A}} = K_p.$$

To verify that inequality (43) guarantees the stability of a compliance-controlled robot interacting with an infinitely stiff environment, a series of tests was performed in which the Minnesota Robot contacted a reinforced aluminum wall, an effectively infinitely stiff environment. To simplify the tests, motor 2 was locked so that the motion of the robot endpoint was within the horizontal ($x_3 = 0$) plane. A three-dimensional piezoelectric force sensor was mounted at the robot endpoint, and numerical transformations were performed by the control computer to resolve endpoint forces into the global Cartesian coordinate frame.

Because motion was confined to the horizontal plane, $H(s)$ was a 2×2 matrix operating on the global, x_1, x_2, contact forces. In all experiments, the compliance compensator H was chosen to supplement compliancy in the normal or x_2 direction.

$$H = \begin{bmatrix} 0 & 0 \\ 0 & \dfrac{H_0}{(s/\omega) + 1} \end{bmatrix}. \tag{45}$$

H was also implemented digitally using the matched pole-zero method. The sampling time was 7.97 ms. ω was empirically chosen to filter high-frequency noise from the force signal and was fixed as 20 rad/s throughout all experiments. By taking the $\hat{A}$ of H, $\alpha_H = H_0$, inequality (43) can be rearranged as

$$H_0 < \frac{1}{\alpha_{JI}^2 \alpha_M K_p} = 1.98 \times 10^{-5} \text{ m/N}. \tag{46}$$

This inequality guarantees that manipulator stability if the gain H_0 of the compliance compensator is less than 1.98×10^{-5} m/N. If the H_0 is set higher than this constant, no conclusions based on (46) can be made.

In the first series of experiments, the robot was command to move along a straight-line Cartesian trajectory intersecting a wall surface (Fig. 7). Throughout the maneuver, the robot approximately followed the command trajectory in the x_1 direction (Fig. 8). As shown in Fig. 9, the robot followed the commanded x_2 trajectory during the unconstrained portion of the maneuver and followed the wall after a brief rebound.

In the first experiment of this series, H_0 was chosen to be 1.9×10^{-5} m/N, satisfying the stability condition in inequality (46). Fig. 10 shows that the system is stable when interacting with the wall. In another set of experiments, H_0 was set to 5.0×10^{-4} m/N. The results are shown in Fig. 11. They verified that the compliance compensator violates the stability

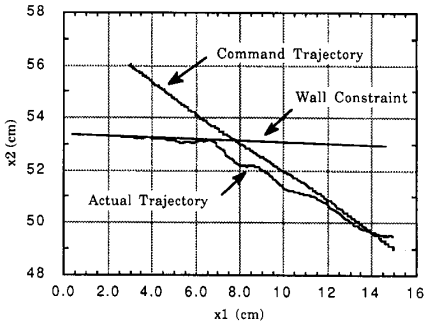

Fig. 7. Graph of command and actual trajectory of the robot endpoint in the x_1-x_2 plane. The command trajectory intersects the wall's surface. The robot approximately follows the command trajectory during the unconstrained portion of the movement. After the initial contact, the manipulator rebounds from the wall due to the impact force. The robot follows the wall surface once contact is restored.

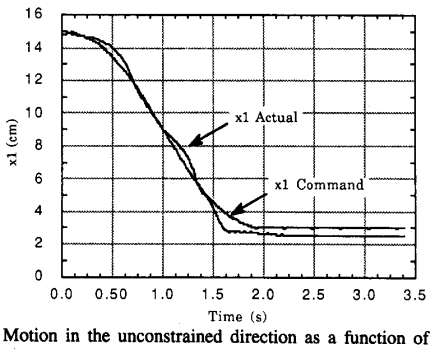

Fig. 8. Motion in the unconstrained direction as a function of time. The actual motion in the x_1 direction approximately follows the commanded motion.

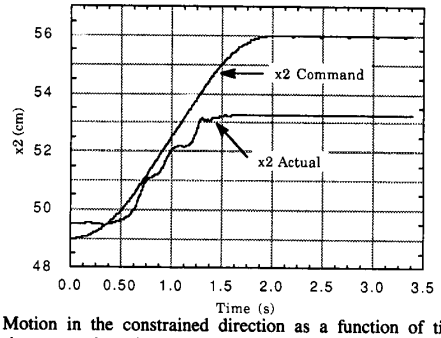

Fig. 9. Motion in the constrained direction as a function of time. The actual motion approximately follows the commanded motion until contact occurs at $t = 1.3$ s; therefore, motion in the x_2 direction is constrained by the wall.

criterion when unstable contact, as indicated by the unbounded contact force, occurs. Finally, the third experiment (Fig. 12), where H_0 was set to 1.0×10^{-4} m/N, violated the stability criterion; yet the system was stable. This experiment illustrated that failure to satisfy the stability criterion does not imply that the system will be unstable and, moreover, showed that inequality (43) defines a conservative stability bound for the compliance compensator H.

VIII. Summary and Conclusions

We have derived three stability conditions: two criteria guarantee stability when a robot interacts with a finite-stiffness

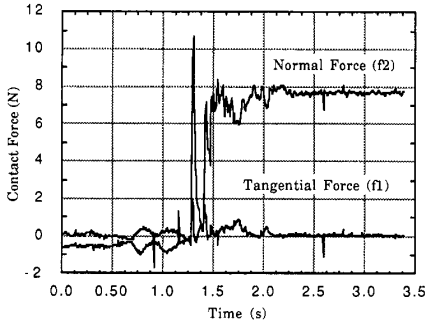

Fig. 10. Stable contact forces for $H_0 = 1.9 \times 10^{-5}$ m/N. Compliance compensator satisfies inequality (46).

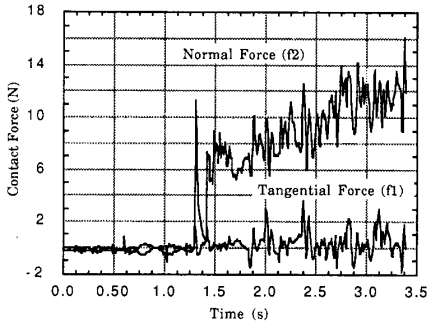

Fig. 11. Unstable contact forces for $H_0 = 5 \times 10^{-4}$ m/N. Compliance compensator violates inequality (46).

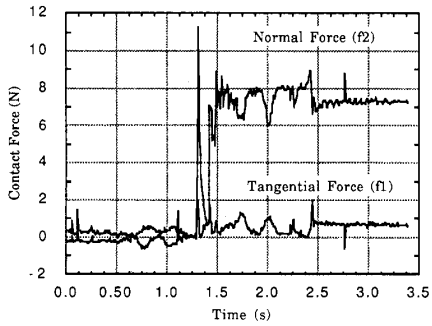

Fig. 12. Contact forces for $H_0 = 1 \times 10^{-4}$ m/N. Manipulator is stable despite the violation of inequality (46).

environment, and the third criterion guarantees stability when a compliance-controlled robot interacts with an infinite-stiffness environment. The first criterion establishes a condition for the stability of a robot and environment when force is not measured for feedback. The first criterion [see (26)] may be simplified to guarantee manipulator stability in unconstrained maneuvers by assuming the environment stiffness is zero. It is shown that the position gain of a PD trajectory compensator must increase in proportion to the environment's stiffness; interaction with a stiffer environment requires a larger position gain to guarantee stability than with a less stiff environment. The second stability criterion represents a stability condition when force feedback has been used to modulate the contact forces. In order to guarantee stability for a given trajectory compensator, the gain of the force compensator H must decrease as the environment's stiffness increases and must be zero if the manipulator operates in the vicinity of a singular point.

A set of experiments was performed to verify the criterion guaranteeing the stability of a manipulator interacting with an infinite stiffness environment [see inequality (43)]. All impact forces were eliminated by commanding the manipulator to move along a path located behind a reinforced aluminum wall. These tests conformed to the assumptions of the stability criterion and demonstrated the sufficiency of the condition. The compensator satisfying the criterion produced stable manipulation, and the compensator that produced unstable manipulation did not.

Appendix A
Mathematical Conventions

1) The L_∞ norm of an $n \times 1$ vector function $f(t)$ is defined as [20]

$$\| f \|_\infty \triangleq \sup_{t \geq 0} \| f(t) \| \tag{A1}$$

where $\| f(t) \|$ denotes the Euclidean norm. If $\| f \|_\infty \leq \infty$, then we say that $f \in L_\infty^n$. For functions that may grow unboundedly, a truncated L_∞ norm is defined as

$$\| f \|_{T\infty} \triangleq \sup \| f(t) \|, \qquad t \geq 0 \text{ and } t < T. \tag{A2}$$

2) H is a L_∞ stable operator if

I) $g = H(f) \in L_\infty^n$ whenever $f \in L_\infty^n$

and

II) $$\| g \|_\infty = \| H(f) \|_\infty \leq \gamma \| f \|_\infty + \beta \tag{A3}$$

where γ denotes the L_∞ norm of H and, loosely speaking, represents the "gain" of H [20]. Note that the symbolism $H(\cdot)$: $L_\infty^n \to L_\infty^n$ may be interpreted as "the function H maps a bounded input f to a bounded output g."

3) If H is a linear operator, then the output $g(t)$, will be equal to the convolution of $h(t)$, the impulse response of $H(s)$, and $f(t)$. For brevity, we use the following shorthand convention throughout the paper for convolution:

$$g(t) = H^*(f). \tag{A4}$$

The L_∞ gain of H is characterized by the $\hat{A}$ norm, which is defined as [20]

$$\| H \|_{\hat{A}} = \sup \frac{\| H^* f \|_\infty}{\| f \|_\infty}, \qquad f \neq 0 \tag{A5}$$

where f is an input vector. The following property of the $\hat{A}$ norm is true [20]:

$$\| H^* f \|_\infty \leq \| H \|_{\hat{A}} \| f \|_\infty, \qquad f \in L_\infty^n. \tag{A6}$$

The $\hat{A}$ norm is computed as follows. Assuming $H(s)$ is strictly proper,[6] the impulse response of $H(s)$ is the inverse Laplace transform matrix $h(t)$ whose elements are scalar functions of time. If all eigenvalues of $H(s)$ have negative real components, the norm $\| H \|_{\hat{A}}$ is defined by [20]

$$\| H \|_{\hat{A}} = \int_0^\infty \| h(t) \| \, dt. \tag{A7}$$

For a scalar system, $h(t)$ is a scalar function and the above equation reduces to

$$\| H \|_{\hat{A}} = \| h(t) \|_1 = \int_0^\infty | f | \, dt. \tag{A8}$$

[6] $H(s)$ has more poles than transmission zeroes.

4) The induced matrix norm is given by

$$\| A \|_\infty \triangleq \max_i \sum_{j=1}^n | a_{ij} | \tag{A9}$$

where a_{ij}'s are the matrix members.

Appendix B

Lemma: Under the given conditions, ξ is L_∞ stable. The truncated L_∞ norm of both sides of (7) is given by

$$\| \xi \|_{T\infty} \leq \alpha_{M1} \| \phi \|_{T\infty} + \alpha_{M2} \| \Delta C \|_{T\infty}, \qquad \forall t \in [0, T] \tag{B1}$$

where α_{M1} is defined in (8) and α_{M2} is defined after inequality (23). Substituting for $\| \phi \|_{T\infty}$ from inequality (4) into (B1) results in

$$\| \xi \|_{T\infty} \leq \alpha_{M1} \alpha_K (\| q_e \|_{T\infty} + \| q \|_{T\infty} + \| p \|_{T\infty}) + \alpha_{M2} \| \Delta C \|_{T\infty}. \tag{B2}$$

Substituting for $\| q_e \|_{T\infty}$, $\| q \|_{T\infty}$, $\| p \|_{T\infty}$ and $\| \Delta C \|_{T\infty}$ into (B2) results in

$$\| \xi \|_{T\infty} \leq \alpha_\xi \| q \|_{T\infty} + \beta_\xi, \qquad \forall t \in [0, T] \tag{B3}$$

where $\alpha_\xi = \alpha_{M1} \alpha_K$ and $\beta_\xi = \alpha_{M1} \alpha_K \alpha_{qe} + \alpha_{M1} \alpha_K \alpha_p + \alpha_{M2} \alpha_{\Delta C}$. Inequality (B3) shows that $\xi(\cdot)$ is bounded over $[0, T]$. Because this reasoning is valid for every finite T, it follows that $\xi \in L_{\infty e}^n$ if $q \in L_{\infty e}^{2n}$. Suppose $q \in L_\infty^{2n}$; then, by using the same reasoning as before

$$\| \xi \|_\infty \leq \alpha_\xi \| q \|_\infty + \beta_\xi, \qquad \forall t \in [0, \infty). \tag{B4}$$

The right-hand side of inequality (B4) is independent of T, and, therefore, inequality (B4) demonstrates the L_∞ stability of the mapping ξ.

Appendix C

Lemma: Under the given conditions, Δq is L_∞ stable. The truncated L_∞ norm of both sides of (30) is given by

$$\| \Delta q \|_{T\infty} \leq \alpha_{JI} \alpha_H (\| f \|_{T\infty} + \| m \|_{T\infty}), \qquad \forall t \in [0, T] \tag{C1}$$

where $\alpha_h \triangleq \| H \|_{\hat{A}}$ and $\alpha_{JI} \triangleq \| J^{-1} \|_\infty < \infty$. Substituting inequality (20) into (C1) results in

$$\| \Delta q \|_{T\infty} \leq \alpha_{\Delta q} \| q \|_\infty + \beta_{\Delta q}, \qquad \forall t \in [0, T] \tag{C2}$$

where $\alpha_{\Delta q} = \alpha_{JI} \alpha_H \alpha_{E1} \alpha_{Kin}$ and $\beta_{\Delta q} = \alpha_{JI} \alpha_H (\alpha_{E2} \| x_0 \|_\infty + \alpha_{E1} \beta_{Kin} + \beta_E + \alpha_m)$. The remainder of the proof is similar to the proof in Appendix B; therefore,

$$\| \Delta q \|_\infty \leq \alpha_{\Delta q} \| q \|_\infty + \beta_{\Delta q}, \qquad \forall t \in [0, \infty). \tag{C2}$$

References

[1] C. H. An and J. M. Hollerbach, "Dynamic stability issues in force control of manipulators," in *Proc. IEEE Int. Conf. Robotics Automat.* (Raleigh, NC), Mar. 1987, pp. 890–896.

[2] J. E. Colgate and N. Hogan, "Robust control of dynamically interacting systems," *Int. J. Control*, vol. 48, no. 1, July 1988.

[3] J. E. Colgate, "The control of dynamically interacting systems," Ph.D. dissertation, Dept. of Mechanical Engineering, M.I.T., Cambridge, MA, Aug. 1988.

[4] N. Hogan "Impedance control: An approach to manipulation, Part I—Theory, Part II—Implementation, Part III—Applications," *ASME J. Dyn. Syst. Meas. Contr.*, pp. 1-24, June 1985.

[5] ——, "On the stability of manipulators performing contact tasks," *IEEE J. Robotics Automat.*, vol. 4, no. 6, Dec. 1988.
[6] H. Kazerooni, "On the robot compliant motion control," *ASME J. Dyn. Syst. Meas. Contr.*, vol. 111, no. 3, Sept. 1989.
[7] ——, "Fundamentals of robust compliant motion of manipulators," *IEEE J. Robotics Automat.*, vol. RA-2, no. 2, 1986.
[8] ——, "On the contact instability of the robots when constrained by rigid environments," *IEEE Trans. Automat. Contr.*, vol. 35, no. 6, June 1990.
[9] H. Kazerooni, B. J. Waibel, and S. Kim, "Theory and experiments on robot compliant motion control," *ASME J. Dyn. Syst. Meas. Contr.*, Sept. 1990.
[10] H. Kazerooni, "Statically balanced direct drive robot manipulator," *Robotica*, vol. 7, no. 2, Apr. 1989.
[11] H. Kazerooni and S. Kim, "A new architecture for direct drive robots," in *Proc. IEEE Int. Conf. Robotics Automat.* (Philadelphia, PA), July 1988, pp. 442–445.
[12] M. T. Mason, "Compliance and force control for computer controlled manipulators," *IEEE Trans. Syst. Man Cyber.*, vol. SMC-11, no. 6, pp. 418–432, 1981.
[13] N. H. McClamroch and D. Wang, "Feedback stabilization and tracking of constrained robots," *IEEE Trans. Automat. Contr.*, vol. 33, no. 5, May 1988.
[14] ——, "Feedback control of position and contact force for a two-dimensional mechanism constrained to a given planar contour," presented at the Amer. Contr. Conf., Atlanta, GA, June 1988.
[15] J. K. Mills and A. A. Goldenberg, "Force and position control of manipulators during constrained motion tasks," *IEEE Trans. Robotics Automat.*, vol. 5, no. 1, Feb. 1989.
[16] M. H. Raibert and J. J. Craig, "Hybrid position force control of manipulators," *ASME J. Dyn. Syst. Meas. Contr.*, vol. 102, pp. 126–133, 1981.
[17] K. J. Salisbury, "Active stiffness control of a manipulator in Cartesian coordinates," in *Proc. 19th IEEE Conf. Decision Contr.* (Albuquerque, NM), Dec. 1980, pp. 95–100.
[18] H. Seraji, "Adaptive force and position control of manipulators," *J. Robotic Syst.*, vol. 4, no. 4, pp. 551–578, 1987.
[19] M. W. Spong and M. Vidyasagar, "Robust nonlinear control of robot manipulators," in *Proc. 24th IEEE Conf. Decision Contr.* (Ft. Lauderdale, FL), Dec. 1985, pp. 1767–1772.
[20] M. Vidyasagar, *Nonlinear Systems Analysis*. Englewood Cliffs, NJ: Prentice-Hall, 1978.
[21] D. E. Whitney, "Historical perspective and state of the art in robot force control," *Int. J. Robotics Res.*, vol. 6, no. 1, pp. 3–14, 1987.

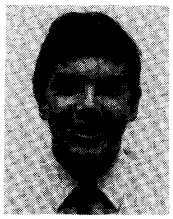

Brian J. Waibel received the Sc.B. (Honors) degree in biomedical engineering from Brown University, Providence, RI, in 1987 and the M.S. degree in mechanical engineering from the University of Minnesota, Minneapolis, in 1989.

He currently operates Waibel Technical Computing in Newark, DE, a consulting firm specializing in the creation of custom engineering software.

Mr. Waibel received the Brown University Ionata Award for creativity in engineering in 1987.

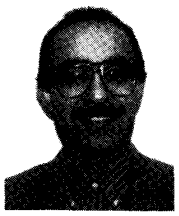

H. Kazerooni (S'84–M'85) received the M.S. degree in mechanical engineering from the University of Wisconsin, Madison, in 1980 and the M.S.M.E. and Sc.D. degrees in mechanical engineering from the Massachusetts Institute Technology, Cambridge, in 1982 and 1984, respectively.

From 1984 to 1985, he was with the Laboratory of Manufacturing and Productivity at the Massachusetts Institute of Technology as a Post Doctoral Fellow. He is currently an Associate Professor in the Mechanical Engineering Department at the University of Minnesota, Minneapolis, where he holds the McKnight-Land Grant Professorship.